TECHNICAL MEMORANDUM

782

Slant path radiative transfer for the assimilation of sounder radiances

Niels Bormann

Research Department

July 2016

European Centre for Medium-Range Weather Forecasts
Europäisches Zentrum für mittelfristige Wettervorhersage
Centre européen pour les prévisions météorologiques à moyen terme

Series: ECMWF Technical Memoranda

A full list of ECMWF Publications can be found on our web site under:
http://www.ecmwf.int/en/research/publications

Contact: library@ecmwf.int

European Centre for Medium-Range Weather Forecasts
Shinfield Park, Reading, RG2 9AX, England

Abstract

This memorandum reports on the influence of taking the slanted satellite viewing geometry better into account in the simulation and assimilation of sounding radiances. The traditional approach is to use a vertical profile extracted at the geo-location information provided with the data. The present work instead investigates using a slanted profile, extracted from model fields along the instrument's line of sight.

Taking the viewing geometry better into account leads to significant improvements in the simulation of brightness temperatures from model fields compared to the traditional approach. This is particularly noticeable for larger zenith angles, for channels that peak in the upper troposphere or higher, and for high and mid-latitudes. The finding also suggests that the model fields capture useful information on horizontal gradients, at least on the relevant spatial scales. The improved simulations of the sounder radiances lead to significant reductions in the size of the analysis increments at mid and high latitudes and particularly in the stratosphere during the assimilation. The system shows a statistically improved self-consistency out to the day-3 forecast range.

1 Introduction

Radiances from microwave or infrared sounders are nowadays the most important observations for Numerical Weather Forecast Systems, both in terms of the number of observations and the forecast impact. During the assimilation, a radiative transfer model is used to convert the atmospheric and surface variables from the forecast model into observation equivalents (e.g., Saunders et al. 1999). Until now, these radiative transfer calculations use a vertical profile of the atmospheric variables, horizontally interpolated to a single latitude/longitude location (e.g., Andersson et al. 1994), neglecting that in reality the satellite's view slants through the atmosphere for all off-nadir views.

In the present memorandum we investigate the effect of taking the satellite viewing geometry better into account during the assimilation of satellite sounding radiances. To our knowledge, it is the first time that this has been evaluated for the assimilation of radiances from so-called nadir sounders. Nevertheless, the effect on radiative transfer calculations has been studied before by Joiner and Poli (2005) and Poli et al. (2005) for AMSU-A and AIRS. They point out that the geo-location error implicit in the current practice is, for instance, around 50 km for observations peaking in the mid-stratosphere and viewed with a zenith angle of 60°. They found that the effect of neglecting the viewing geometry was small (below the instrument noise) for most channels, and, as expected, primarily confined to the higher peaking channels when viewed with the most extreme zenith angles. However, these findings should be revisited, given the advent of sounders with considerably lower noise levels (such as CrIS) and much wider swaths (ie larger maximum zenith angles and more extreme viewing geometries, e.g., CrIS, ATMS). Also, the steady increase in the accuracy of NWP fields and improved horizontal model resolutions mean that we are now better able to describe horizontal gradients in our background fields. We may hence also be more sensitive to the implicit geo-location error introduced through the current practice.

The present study has some similarities with work on taking radiosonde balloon drift into account, reported by Laroche and Sarrazin (2013). They showed considerable benefits in the calculation of observation equivalents and also reported some positive forecast impact. The mean displacements encountered were around 30-40 km around the tropopause, broadly comparable with the displacements encountered in the present study for the largest zenith angles considered. For satellite data, benefits of taking horizontal structure into account have previously been demonstrated for observations that use the limb-viewing geometry. Bormann et al. (2007) used a 2-dimensional operator for the assimilation of limb radiances, showing that such an operator simulates the observations better from model fields compared to an opera-

tor that neglects horizontal structure. They also found further benefits in the assimilation in regions with considerable horizontal gradients. Similarly, Healy et al. (2007) show clear benefits in the simulation of GPS radio occultation bending angles from taking horizontal features into account in a 2-dimensional observation operator. The latter approach has been used operationally at ECMWF since May 2015. Of course, the horizontal extent of the sensitivity of limb-viewing observations is more than an order of magnitude higher than that encountered with downward-looking radiances (1000-2000 km versus up to 50-100 km), so the comparability of the above findings for our present work is fairly limited.

The structure of the present memorandum is as follows: first, we describe the method used, followed by an assessment of the benefits in terms of calculating model equivalents. Results of assimilation experiments are then reported, before we discuss our overall conclusions.

2 Method

The viewing geometry of a so-called nadir sounder is illustrated schematically in Fig. 1. The latitude/longitude of the intersection of the instrument's view with the Earth's geoid is usually provided as geo-location information in the satellite data. When calculating observation equivalents from model fields, current practice at NWP centres is to first interpolate the model fields horizontally to this single latitude/longitude location, and to then perform radiative transfer calculations with the resulting profile. This profile is hence extracted along the red line in Fig. 1. The current practice neglects that in truth the instrument's view slants through the atmosphere (see the blue line in Fig. 1), as given by the satellite's zenith and azimuth angles. Effectively, this means that for higher peaking channels the current practice extracts the model information at the wrong place, and the displacement is most relevant for larger zenith angles and for channels whose weighting functions peak higher in the atmosphere. For example, for a lower stratospheric channel peaking around 16 km and viewing the Earth with a zenith angle of 60°, the weighting function peak will be displaced by around 28 km, and the stratospheric tail of the weighting function will experience even larger displacements. While the displacements are not large compared to the resolution of today's global NWP models, the error can be avoided by making better use of the model atmosphere during the horizontal interpolation.

In the present work, we have modified the spatial interpolation used in the ECMWF assimilation system and instead extract the profile along the satellite's viewing path (ie, the blue line shown in Fig. 1). We simplify the calculation of the viewing path by assuming a plane-parallel atmosphere and neglecting any bending resulting from density gradients in the atmosphere. These simplifications are justified given the relatively small spatial scales involved. The viewing path is then described through the following relationship between the geometric height Δz and the corresponding displacement in the azimuthal plane Δx, given a satellite zenith angle θ:

$$\Delta x = \Delta z \tan(\theta) \tag{1}$$

For the largest zenith angles encountered in the present study and the current model top of around 90 km, the maximum displacement is around 160 km. The slanted profile resulting from the interpolation is subsequently used in the radiative transfer calculations in the same way as the previously interpolated vertical profile.

The modification of the interpolation uses the technical framework developed for the assimilation of limb radiances or GPS radio-occultation measurements (Bormann et al. 2007, Healy et al. 2007), and it proceeds as follows: first, we spatially interpolate the model fields to the vertical plane containing the

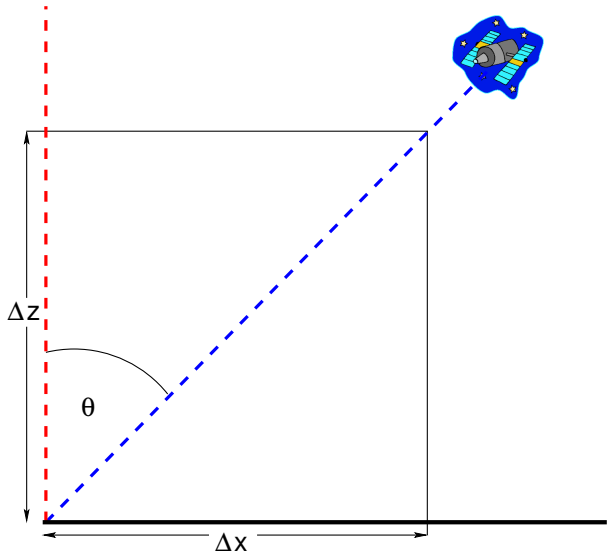

Figure 1: Schematic illustration of the satellite viewing geometry, viewing a location on Earth with a zenith angle of θ along a slanted path through the atmosphere (blue). The vertical profile currently used for radiative transfer calculations is indicated in red.

viewing path, given by the geo-location information and the satellite azimuth angle. This interpolation results in n vertical profiles given on the usual forecast model levels, equally spaced spatially in the azimuthal plane.[1] Next, we use the satellite zenith angle to horizontally interpolate the information from the n profiles to the actual viewing path, using (1). The interpolation is applied to all atmospheric variables (including pressure which is normally determined by the surface pressure through the model's vertical coordinate description). The result is a single profile, on levels corresponding to model levels, representing the atmospheric model information along the viewing path.

In the present work, we use $n = 6$ profiles, with a horizontal spacing of 32 km, to sample the relevant 160 km horizontal extent of the azimuthal plane in all trajectory calculations. The sensitivity of the radiance simulations to the horizontal spacing is investigated in Appendix A. Given the coarser spatial resolution of the incremental analysis, we use instead $n = 3$ profiles with a spacing of 80 km in the minimisation.

3 Improvements in the simulation of observations

We will first investigate the impact of the slant-path approach on the simulation of observation equivalents from model fields, independent of its use during the assimilation. To do so, we simulated observation equivalents from short-range forecasts from the ECMWF system, once in the conventional way by using a vertical profile extracted at the observation location, and once with taking the slant-path geometry into account. We used the same short-range forecast for both simulations, taken from an ECMWF experiment run at $T_{CO}1279$ spatial resolution (≈9.5 km), ie the spatial resolution of the operational ECMWF system since the resolution upgrade on 8 March 2016. We performed these simulations over the period 25

[1] Message-passing is involved in this step, as the processor that owns the observation does not necessarily own the relevant chunk of the atmospheric model fields. Subsequent processing can then be performed on the processor that owns the observation.

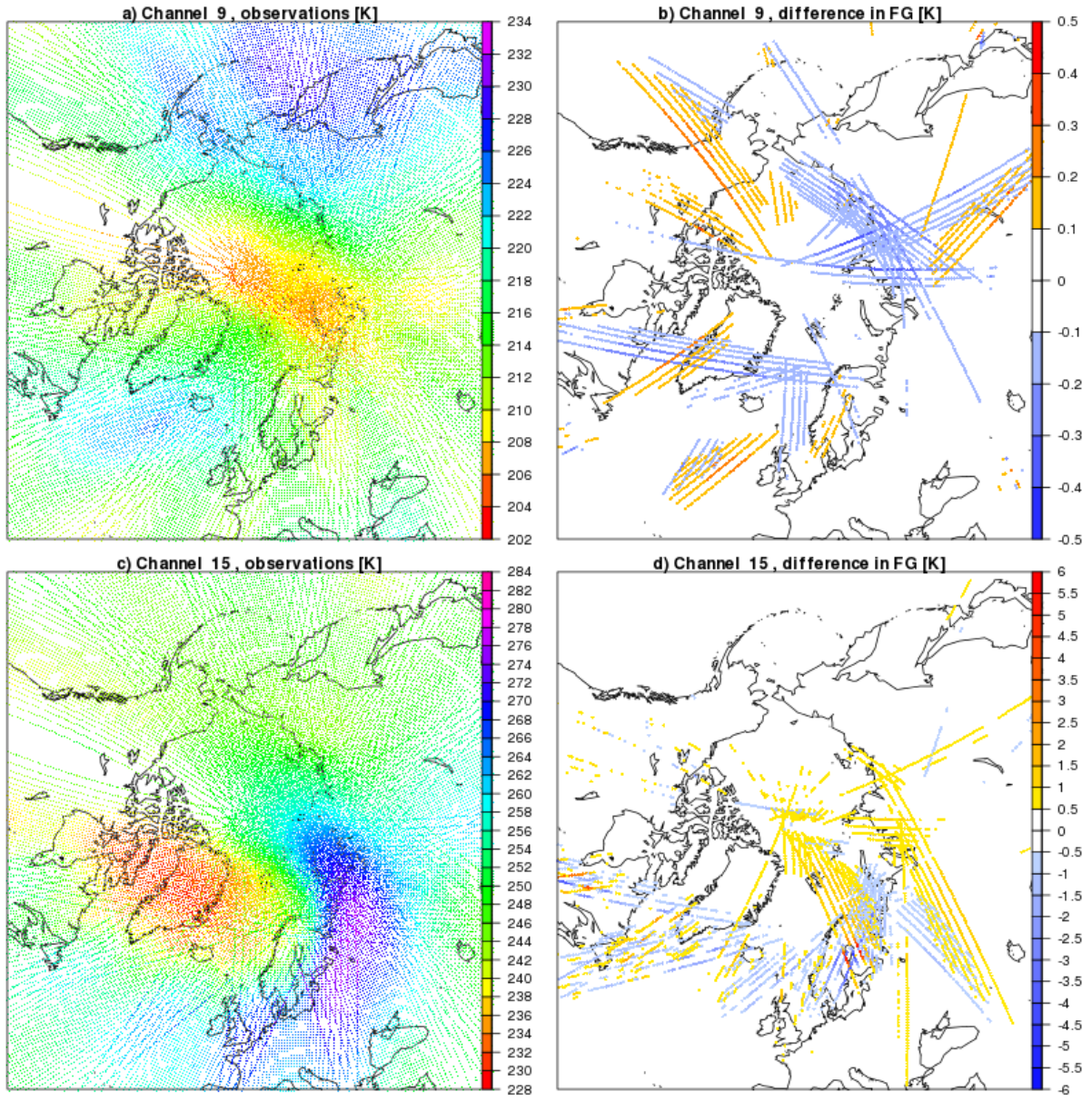

Figure 2: a) Observed brightness temperatures [K] for ATMS channel 9 for a 12-hour period around 25 January 2015 00UTC. b) Difference in the radiative transfer simulations from short range forecasts with and without taking the slant-path effect into account, for the observations shown in a). Note that only differences with an absolute value larger than 0.1 K are shown. c) As a), but for channel 15 of ATMS. d) As b), but for the observations shown in c). Note that only differences with an absolute value larger than 0.5 K are shown here.

January – 24 February 2015. We focus here initially on the impact on ATMS, given the particularly wide swath of this instrument, but other instruments are also considered later. Note that we use ATMS observations here as in the ECMWF system, that is, after averaging observations from 3 neighbouring scan-positions and 3 neighbouring scan-lines (so-called "3×3 averaging"; see Bormann et al. 2013 for further details on the assimilation of ATMS data at ECMWF).

The difference between the two approaches is illustrated in Fig. 2b and c for a sample case for two

selected channels. As can be seen, the differences can reach almost ±0.5 K for channel 9, a temperature-sounding channel peaking around the tropopause, and locally they even exceed 5 K for channel 15, the top-most temperature sounding channel of ATMS, peaking around 2 hPa. These are sizeable differences in the radiative transfer calculations for these channels that typically show standard deviations of observation minus background departures of around 0.14 K and 0.9 K, respectively. As expected, the differences are mainly confined to the edges of the swath, where satellite zenith angles are largest. Differences also only become sizeable when the observations indicate a significant spatial gradient along the azimuthal direction (which is approximately cross-track for ATMS), such as the gradients over the Gulf of Bothnia for channel 15 in Fig. 2d. In such regions, the differences are, by nature, spatially correlated for scan-positions with larger zenith angles. Where spatial gradients are small, the differences between the two approaches are also small. It is also apparent that the difference in treating the viewing geometry can lead to differences in the simulations of the opposite sign for two different over-passes, as encountered over Greenland for channel 9 (Fig. 2b).

The dependence of the impact of the slant-path calculations on the zenith angle is further characterised through comparisons with observations in Fig. 3. Fig. 3a shows very significant reductions in the standard deviation of the differences between observations and model equivalents for the outer-most scan positions of up to 17 % for channel 9. The weighting function of channel 9 peaks at around 16 km, so typical displacements around the weighting function peak are about 28 km for the outermost scan-positions according to (1), but the stratospheric tail of the weighting function will be displaced further. Note that these outer scan-positions also show considerably larger departures than the scan-positions with small zenith angles in the conventional approach, whereas this effect is much reduced when the viewing geometry is better taken into account. It appears that the conventional approach introduces a sizeable error in the observation operator calculations for these observations. The impact is qualitatively the same

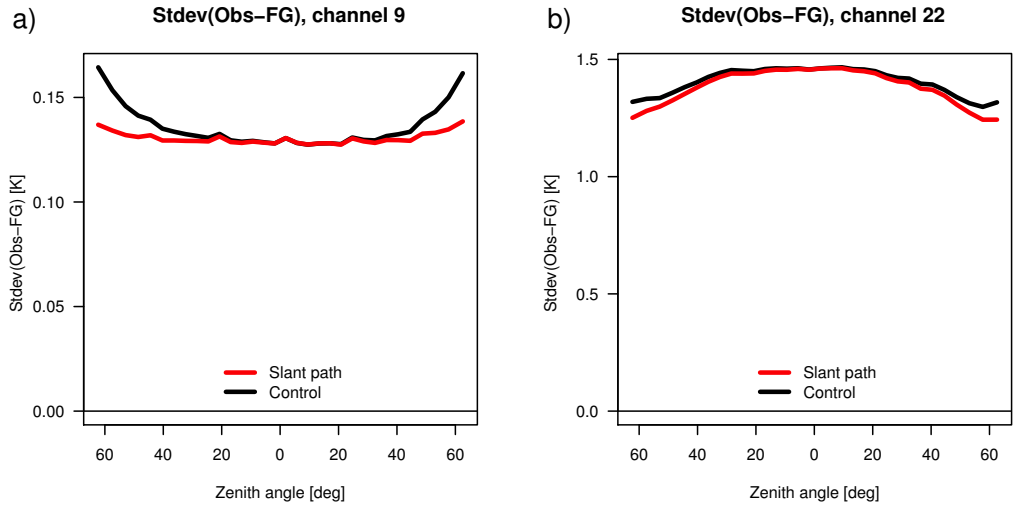

Figure 3: a) Standard deviations of differences between observations and short-range forecast equivalents for channel 9 of ATMS as a function of the scan position (labelled here with the average satellite zenith angle). Black indicates the conventional treatment, red indicates statistics for calculations that take the slant-path geometry into account. The statistics cover the period 25 January to 24 February 2015, and are based on data over sea after cloud/rain screening. Biases have been removed based on bias corrections obtained from the underlying assimilation experiment that uses the conventional radiative transfer simulations. b) As a), but for channel 22 of ATMS, the highest peaking humidity sounding channel.

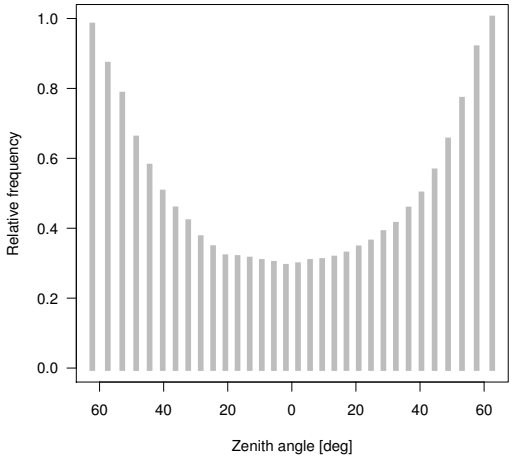

Figure 4: Number of observations after geophysical quality control and after spatial thinning as a function of scan-position (labelled here by average zenith angle) for ATMS.

for all temperature-sounding channels, but the upper stratospheric channels still show some increase in the standard deviations for the outer scan-positions even when the slant path geometry is taken into account.

The humidity-sounding channels of ATMS also show a reduction in the standard deviation of the differences between observations and model equivalents for the outer-most scan positions (e.g., Fig. 3b for channel 22, the highest ATMS humidity sounding channel). The relative reduction in the standard deviations of departures is not as large, partly because the channel is primarily sensitive to the upper troposphere (ie, lower than the temperature-sounding channel shown in Fig. 3a), and partly due to the larger influence of short-range forecast errors. This channel also does not show larger standard deviations for the outer scan-positions in comparison to the central scan-positions when the conventional approach is used. This is most likely because other aspects are dominating the behaviour in this case, for instance, the performance of the cloud detection.

It is worth noting here that after spatial thinning, relatively more observations from the outer scan-positions are selected in the ECMWF system (e.g., Fig. 4), making the improvements demonstrated here even more relevant. This is because for today's cross-track sounders the steps between scan-positions are constant in the viewing angle, resulting in spatial sampling that is finer for near-nadir-looking scan-positions and further apart for outer scan-positions. The spatial thinning applied to the data then selects one observation per spatial thinning box, and hence thins out more data where the samples are closer together, that is, for the near-nadir viewing scan-positions.

For temperature-sounding channels, the influence of performing the slant-path calculations is most relevant at mid and high latitudes, where gradients along the azimuthal direction are largest. This is shown, for instance for channel 9 in Fig. 5a which highlights considerable reductions in the standard deviation of the differences between observations and simulations from the short-range forecasts in these regions. For the higher humidity sounding channels, the reduction of the standard deviations is most noticeable around the mid-latitude storm-tracks (see, for instance, Fig. 5b). Some small effect on the geographical bias pattern can also be found (e.g., Fig. 6), and these will lead to small adjustments in the variational bias correction applied to these data during the assimilation. However, the mean changes are relatively small in comparison to the standard deviation of departures or the geographical variation of residual biases pattern that tend to be present after bias correction.

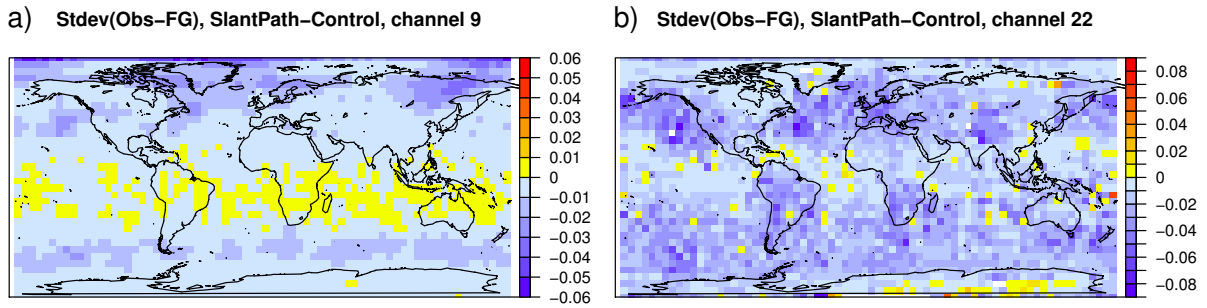

Figure 5: a) Maps of the difference in the standard deviations of the departures [K] for channel 9 of ATMS between taking the slant-path geometry into account and neglecting the slant-path geometry. Negative values indicate a reduction in the standard deviations from taking the slant-path geometry into account. Statistics are based on simulations from the same short-range forecasts, covering the period 25 January to 24 February 2015, after geophysical quality control. Biases have been removed based on bias corrections obtained from the underlying assimilation experiment that uses the conventional radiative transfer simulations. b) As a), but for channel 22.

Looking at the effect for other instruments, Fig. 7 shows that the slant-path modelling improves the radiative transfer calculations for all sounding instruments considered here, as can be seen from reductions in the standard deviations of observation departures. ATMS and CrIS show the largest benefits from the slant-path modelling, with relative reductions reaching, respectively, 8 % and 2 % globally. This is the result of relatively wide swaths with large maximum zenith angles, combined with lower noise in the observations, so that these effects are relatively more important. For the other instruments, the reductions in the standard deviations stay typically below 1 % globally, but reductions for high zenith angles at higher latitudes are of course significantly larger than that. For AIRS and AMSU-A, these findings are in line with those reported by Joiner and Poli (2005). Another aspect is noticeable in these statistics: In absolute terms, the influence of taking the slanted path into account will be larger the higher the channel peaks in the atmosphere. However, this is not necessarily the case for these relative statistics. Aside from differences in the instrument noise for some of these channels, this also reflects that errors in the short-range forecasts are also larger for channels that peak in the stratosphere, so the relative effect is not as pronounced.

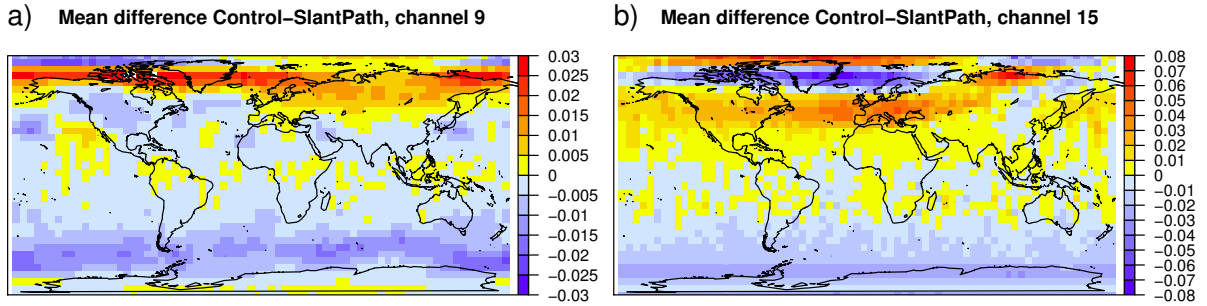

Figure 6: a) Maps of the mean difference [K] between neglecting the slant-path geometry and taking it into account in the simulations from short-range forecasts for channel 9 of ATMS on S-NPP. Statistics are based on simulations from the same short-range forecasts, covering the period 25 January to 24 February 2015, after geophysical quality control applied to the underlying observations. b) As a), but for channel 22.

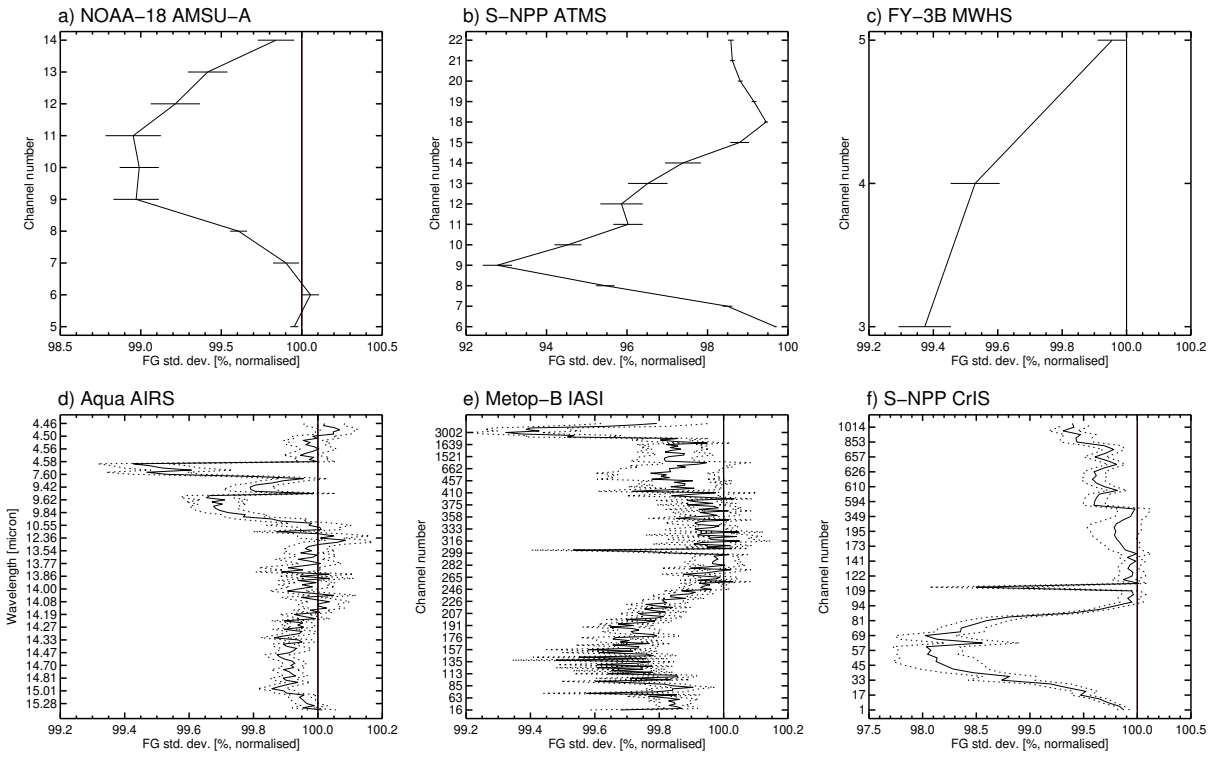

Figure 7: Standard deviation of differences between observations and simulations that take the slant-path geometry into account, normalised by equivalent values obtained with simulations that ignore the slant-path geometry. Values below 100 % indicate smaller standard deviations when the slant-path geometry is taken into account. Horizontal bars indicate 95 % significance intervals. Statistics are based on data covering the period 25 January to 24 February 2015, after quality control and thinning and after applying bias correction. The six panels show: a) Statistics for AMSU-A on NOAA-18, b) ATMS on S-NPP, c) MWHS on FY-3B, d) AIRS on Aqua, e) IASI on Metop-B, and f) CrIS on S-NPP.

4 Results from assimilation experiments

We will now report on assimilation experiments designed to investigate the effect of taking the slant-path geometry into account. We conducted two assimilation experiments: a Control that neglects the slant-path effect, similar to the ECMWF operational configuration, and a SlantPath experiment, in which the slant-path effect is taken into account for all sounder radiances that are not treated in the all-sky system, that is: AMSU-A, ATMS, MWHS, HIRS, AIRS, IASI, CrIS. The experiments use ECMWF's 12-hour 4DVAR assimilation system, with a model resolution of $T_{CO}639$ ($\approx$ 16 km), an incremental analysis resolution of T_L255 ($\approx$ 80 km), and 137 levels in the vertical. The experiments were conducted over the two four-month periods 2 June - 30 September 2014 and 2 December 2014 - 31 March 2015.

The most notable effect for the assimilation experiments is a very significant reduction in the size of the analysis increments, by up to around 10 % at higher latitudes and higher levels. This is illustrated in Fig. 8a which shows zonal mean normalised differences in the standard deviation of analysis increments for wind. Other variables show a very similar pattern. As we did not change the observation errors used in the present experiments, this reduction is an expected effect of the smaller departures for the sounder radiances shown in the previous section. It could of course be argued that the reduction in the observation operator error apparent from the previous section means that the assumed observation

error used in these experiments should be reduced accordingly for the affected observations. We have not pursued this here, as the uncertainty in the assumed observation errors is probably larger than the reduction in the observation operator error obtained with the present modification. However, the present change may well contribute to allowing the use of a reduced observation error, for instance for ATMS, and this aspect could be studied further.

The reduction in the size of the increments is not accompanied with sizeable reductions in the FG departures for other assimilated observations. While GPS RO, radiosonde temperatures or the upper-most MHS or SSMIS humidity sounding channel show statistically significant reductions in the affected geographical regions, they remain at most at 0.1-0.2 % when averaged over the extra-tropics. These are hence very small improvements (not shown). This may suggest that the impact on the quality of the FG is not very large. Departure statistics for sounder radiances are dominated by the very significant reductions in the size of the FG-departures as shown in Fig. 7, a result of reduced errors in the observation operator, rather than an indication of an improved short-range forecast. Improvements beyond that are difficult to ascertain.

The reduced analysis increments lead to some statistically significant reductions in the size of the forecast

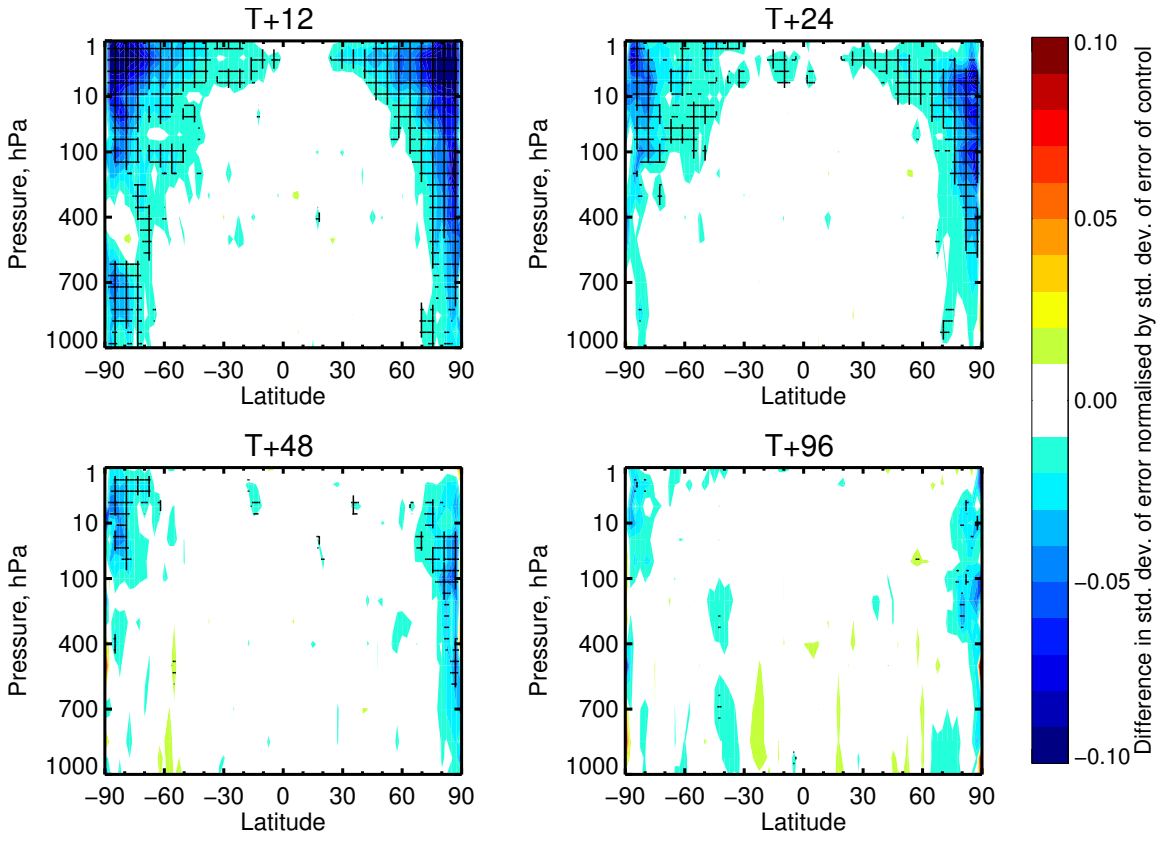

Figure 8: a) Zonal means of normalised differences in the standard deviation of vector wind analysis increments between the SlantPath experiment and the Control. Blue indicates a reduction in the standard deviation of the increments in the SlantPath experiment compared to the Control. Cross-hatching marks statistical significance at the 95 % confidence level. b) As a), but for the 24-hour forecast verified against its own analysis. c) As b), but for the 2-day forecast. d) As a), but for the 3-day forecast. All statistics cover approximately 8 months over the two seasons combined, with a total of 430 to 468 samples.

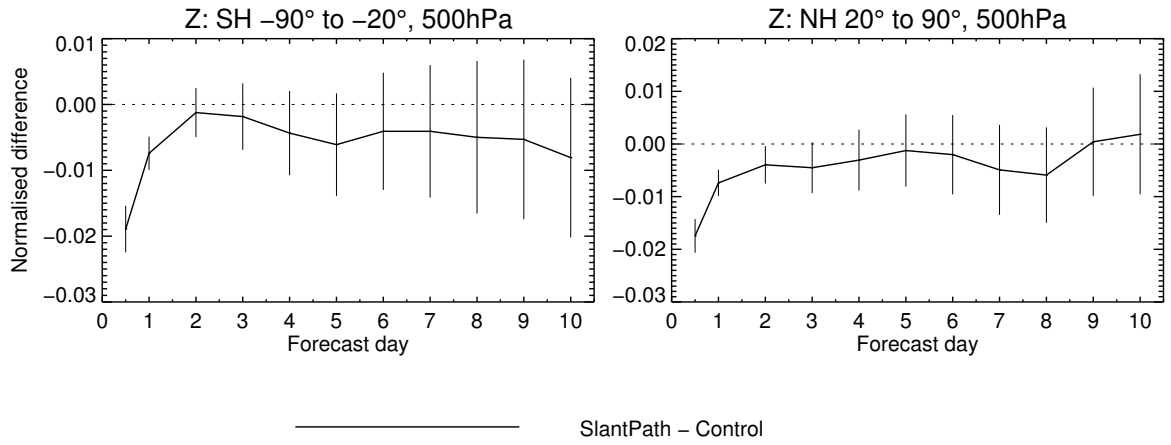

Figure 9: Normalised difference in the standard deviation of forecast errors in the 500 hPa geopotential as verified against each experiment's own analysis for the Southern Hemisphere extra-tropics (left) and the Northern Hemisphere extra-tropics (right). Vertical bars indicate 95 % significance intervals.

errors up to day 3 when each experiment is verified against its own analysis (e.g., Fig. 8b-c). However, these reductions beyond day 1 are mostly small and generally less than 1 % when averaged over the extra-tropics in the troposphere (e.g., Fig. 9). For the stratosphere, some statistically significant benefits can be found out to the day four forecast at high latitudes. Nevertheless, it appears that the observation operator errors present in the Control due to neglecting the slant-path effect have a relatively limited effect on forecast quality in the medium range.

5 Conclusions

In this memorandum we investigated taking the satellite viewing geometry better into account in the observation operator for most sounder radiances in the ECMWF assimilation system (AMSU-A, ATMS, MWHS, HIRS, AIRS, IASI, CrIS). The main findings are:

- Neglecting the slant-path geometry adds a significant error to the radiative transfer simulations for larger zenith angles. Compared to typical background errors and instrument noise contributions, this error is particularly relevant for temperature-sounding channels, especially around the upper troposphere/lower stratosphere, but it is also apparent for humidity sounding channels.

- The slant path effect is most noticeable at mid and higher latitudes for temperature-sounding channels and for the mid-latitudes for humidity-sounding channels.

- Taking the viewing geometry into account for most sounder radiances (without changes to the assigned observation errors) leads to very significant reductions in the analysis increments, particularly at high latitudes and in the upper stratosphere.

- The forecast impact of taking the viewing geometry into account is most noticeable in the stratosphere, particularly at high latitudes, whereas over the troposphere it is primarily limited to the first 3 days and the high latitudes.

The present study is an example of making better use of the full 3-dimensional description of the atmosphere available in an assimilation system, which leads to clear benefits in the simulation of observation-equivalents. However, the medium-range forecast impact of this modification is rather small, suggesting that the current practice of neglecting the slant-path effect is not a major limitation. At the same time, there are aspects that have not been studied here, and they could further enhance the forecast impact: 1) The reduction in the observation operator error achieved here has not been reflected in the assigned observation errors, which have been left unaltered. This is partly because the observation errors assigned in these experiments do not explicitly aim to model the statistical properties of this effect (e.g., through a scan-position-dependent parameterisation), and partly because the uncertainty in the assigned observation errors is considered larger than the reduction in the observation operator error achieved here. Nevertheless, it is clear that at least for some instruments such as ATMS, the error due to neglecting the slant-path effect is considerable for certain conditions, and the elimination of this error source should help to be able to assign lower observation errors in the future. This may lead to more benefits in terms of forecast impact. 2) The slant-path effect has not been taken into account for instruments treated in the all-sky system, that is MHS, SSMIS, and the microwave imagers. This is primarily because simple interpolation of cloud-affected fields to the slant-path may be less appropriate, and this aspect deserves special attention. While the slant-path effect may not be very relevant for microwave imager channels in any case, the SSMIS sounding channels could benefit more noticeably, as the approximately constant zenith angle of 53.1° is relatively large for all observations for this conical scanner. Taking the slant-path into account is likely to be particularly beneficial for the upper atmosphere sounding channels of SSMIS, some of which peak at around 65 km. Note that these channels are currently not assimilated in the ECMWF system, but could be considered in the future.

It is worth putting the reductions in the observation operator error for sounder radiances seen here into context with other observation operator uncertainties. For microwave sounders, the channel pass-band characteristics add a considerable potential uncertainty, as highlighted, for instance, by Lu and Bell (2014). In addition, uncertainties in the spectroscopy or line-shape modelling can introduce errors, as has been noticeable, for instance, when considering different spectroscopy for hyperspectral infrared instruments (e.g., Bormann et al. 2009, Matricardi 2009, Lupu et al. 2015). Many of these radiative-transfer related uncertainties, however, mostly lead to considerable air-mass dependent biases. The effect on statistics after bias correction tend to be fairly small for revised channel pass-bands or updated spectroscopy, with changes typically of the order of less than 1 % in terms of the global standard deviation of background departures. Compared to this, the overall reductions found in the present study are quite considerable.

Given increasing refinements in the model representation of the atmosphere and smaller errors in short-range forecasts, it is expected that making better use of the full 3-dimensional description of the atmosphere will receive growing attention in the future. A number of avenues could be pursued in this context. For instance, observation operators for sounder radiances could take into account the spatial characteristics of the satellite footprint, in order to better match the representativeness of the model and observations. In the case of all-sky assimilation, the viewing geometry can have considerable effects around clouds, and local 3-dimensional radiative transfer calculations may offer benefits in certain situations. It is expected that these aspects will also lead to further refinements in the treatment of spatial representativeness errors which are closely linked to the present work.

A Choice of horizontal resolution in the azimuthal plane

As described in section 2, the slant-path geometry is taken into account in the present work by interpolating in two steps: First, the full 3-dimensional atmospheric fields are interpolated to a series of vertical profiles which describe a plane given by the geo-location information and the satellite's azimuth angle. Next, this series of profiles is interpolated to the line-of-sight as given by the satellite's zenith angle. The number of profiles used, or, more importantly, the horizontal spacing of the profiles describing the azimuthal plane is a configurable parameter, and in the following we will present results that motivated our choice of using 6 profiles, with a spacing of 32 km in the outer-loops, and 3 profiles with a spacing of 80 km during the minimisation.

To investigate this aspect, we conducted a series of simulations similar to the ones presented in section 3, that is, we simulated brightness temperatures from short-range forecasts and compared them to observations, over the period 20-25 January 2015. The short-range forecasts are the same for all simulations, and they are taken from an assimilation experiment with a $T_{CO}1279$ (≈ 9.5 km) spatial model resolution and a T_L399 (≈ 50 km) incremental analysis resolution. The only aspect that was varied in these simulations was the horizontal spacing of the profiles describing the azimuthal plane, varying from 9.5 km (the resolution of the forecast model underlying these simulations) to 160 km. In all cases, the azimuthal plane covered by the profiles has an extent of 160 km, chosen to be appropriate for the typical maximum zenith angle and the highest model level.

The influence of the horizontal spacing on the departure statistics is summarised in Fig. 10 for a selection of ATMS channels, highlighting that the finest horizontal spacing does not always lead to the smallest departures for the outer scan positions. For the tropospheric and lower stratospheric ATMS temperature channels 6-11, there is hardly any difference whether the azimuthal plane is sampled every 9.5 km or only every 160 km (e.g., Fig. 10a). This probably reflects relatively smooth temperature fields and reliable temperature gradients in the model fields in the troposphere and lower stratosphere. For the upper stratospheric temperature channels, the best agreement with observations is in fact obtained when the azimuthal plane is sampled every 160 km (e.g., Fig. 10b), whereas for the humidity-sounding channels, the best agreement is found for sampling of 80 km (e.g., Fig. 10c). For the upper stratospheric channels and the humidity-sounding channels, the finest sampling leads to *worse* agreement with the observations. This probably suggests that horizontal gradients provided by the model fields at the finest scales are noisy and less reliable for stratospheric temperature or tropospheric humidity. For humidity, it appears that the horizontal gradient information is most reliable if we extract it at scales that are around twice the grid spacing of the incremental analysis. Coarser sampling degrades the available information, but finer sampling appears to add noise. This aspect could be studied further, and the slant-path approach may be a useful tool to characterise at which scales horizontal gradient information from model fields provides useful information.

For the present study, it is clear that sampling the azimuthal plane at the full model resolution brings no benefit, and coarser sampling is adequate and possibly even beneficial. This has obvious computational benefits as well, as it reduces memory requirements and the number of interpolations together with the amount of message-passing that needs to be performed. Our choice of using 32 km horizontal sampling in the outer loop and 80 km spacing the inner loop is a compromise between the desire to use most of the spatial information available from the short-range forecast on the one hand, and the finding that further refinements do not lead to benefits on the other.

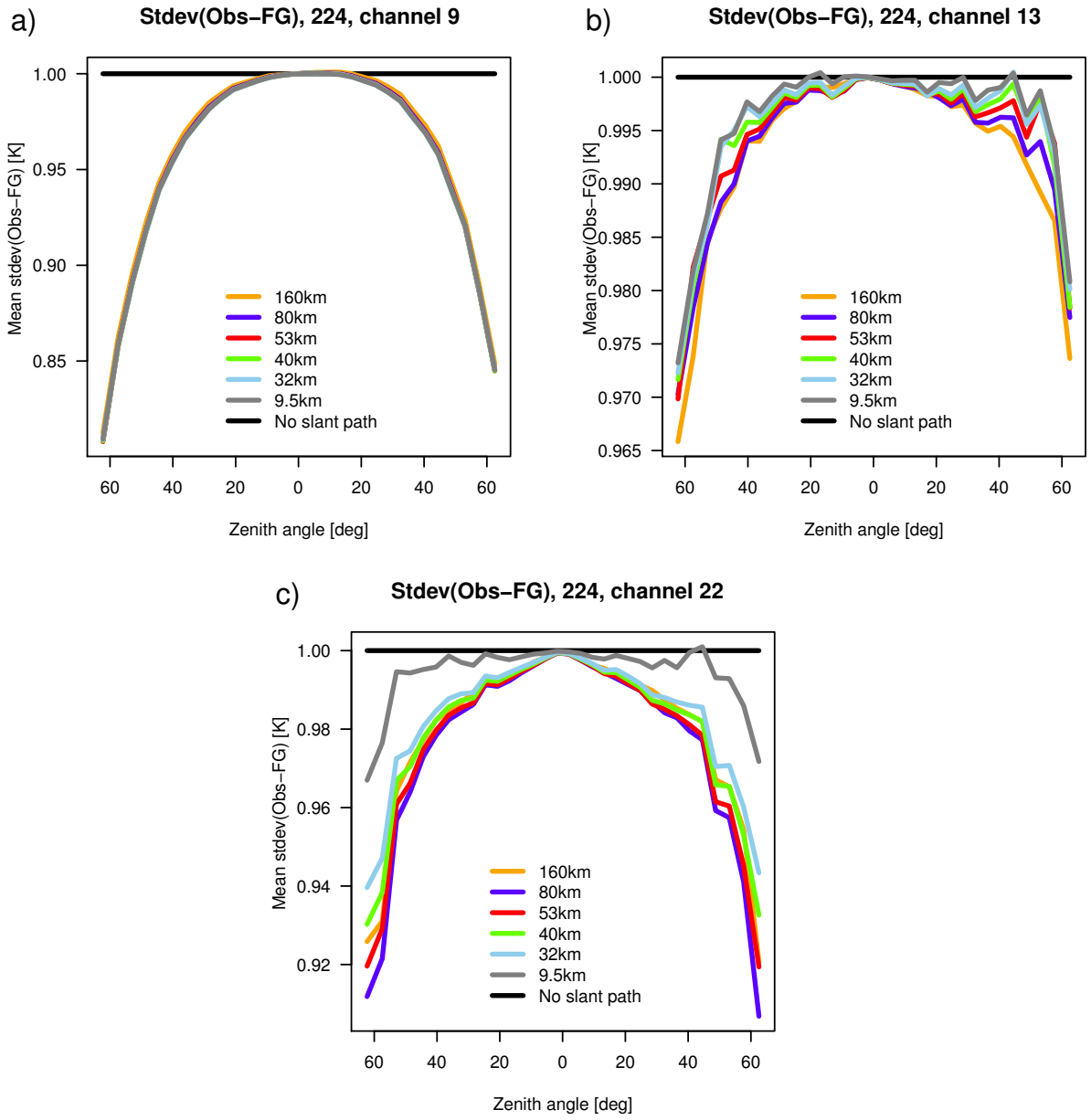

Figure 10: a) Standard deviations of differences between observations and short-range forecast equivalents for channel 9 of ATMS as a function of the scan position (labelled here with the average satellite zenith angle). Black indicates results obtained with the conventional treatment, whereas coloured lines show results where the slant-path geometry has been taken into account, with the profile spacing in the azimuthal plane as indicated in the legend. The statistics cover the period 20-25 January 2015, and are based on data over sea after geophysical quality control. Biases have been removed based on bias corrections obtained from the underlying assimilation experiment that uses the conventional radiative transfer simulations. b) As a), but for channel 13 of ATMS. c) As a), but for channel 22 of ATMS, the highest peaking humidity sounding channel.

Acknowledgements

The technical framework to account for spatial structure in the observation operator was initially developed by Mats Hamrud and more recently substantially re-designed by Alan Geer.

References

Andersson, E., J. Pailleux, J.-N. Thépaut, J. R. Eyre, A. P. McNally, G. A. Kelly, and P. Courtier, 1994: Use of cloud-cleared radiances in three/four-dimensional variational assimilation. *Q. J. R. Meteorol. Soc.*, **120**, 627–653.

Bormann, N., A. Fouilloux, and W. Bell, 2013: Evaluation and assimilation of ATMS data in the ECMWF system. *J. Geophys. Res.*, **118**, 12,970–12,980, doi: 10.1002/2013JD020325.

Bormann, N., S. B. Healy, and M. Hamrud, 2007: Assimilation of MIPAS limb radiances in the ECMWF system. Part II: Experiments with a 2-dimensional observation operator and comparison to retrieval assimilation. *Q. J. R. Meteorol. Soc.*, **133**, 329–346.

Bormann, N., D. Salmond, M. Matricardi, A. Geer, and M. Hamrud, 2009: The RTTOV-9 upgrade for clear-sky radiance assimilation in the IFS. Technical Memorandum 586, ECMWF, Reading, UK, 26 pp [available under www.ecmwf.int/publications/library/do/references/list/14].

Healy, S., J. Eyre, M. Hamrud, and J.-N. Thépaut, 2007: Assimilating GPS radio occultation measurements with two-dimensional bending angle observation operators. *Q. J. R. Meteorol. Soc.*, **133**, 1213–1227.

Joiner, J., and P. Poli, 2005: Note on the effect of horizontal gradients for nadir-viewing microwave and infrared sounders. *Q. J. R. Meteorol. Soc.*, **131**, 1783–1792.

Laroche, S., and R. Sarrazin, 2013: Impact of radiosonde ballon drift on numerical weather prediction and verification. *Weather and Forecasting*, **28**, 772–782.

Lu, Q., and W. Bell, 2014: Characterizing channel center frequencies in AMSU-A and MSU microwave sounding instruments. *J. Atmos. Oceanic Technol.*, **31**, 1713–1732.

Lupu, C., M. Matricardi, and A. McNally, 2015: Monitoring infrared satellite radiance biases using the ecmwf model. In Poster presented at the 20th international TOVS study conference, Lake Geneva, Wisconsin, US, CIMSS, University of Wisonsin, Madison, US, available from http://cimss.ssec.wisc.edu/itwg/itsc/itsc20/program/PDFs/28Oct/session2b/2p_09_lupu.pdf.

Matricardi, M., 2009: Technical note: An assessment of the accuracy of the RTTOV fast radiative transfer model using IASI data. *Atmos.Chem.Phys.*, **9**, 6899–6913.

Poli, P., J. Joiner, and D. Lacroix, 2005: Application of radiative transfer to slanted line-of-sight geometry and evaluation with AIRS data. In Proceedings of the 14th International TOVS Study Conference, Beijing, China, 6.4 [available online: cimss.ssec.wisc.edu/itwg/itsc/itsc14/proceedings/6_4_Poli.pdf].

Saunders, R., M. Matricardi, and P. Brunel, 1999: An improved fast radiative transfer model for assimilation of satellite radiance observations. *Q. J. R. Meteorol. Soc.*, **125**, 1407–1426.